Article ID: 1003－6326(2003)01－0208－05

Numerical calculation and industrial measurements of metal pad velocities in Hall-Heroult cells①

ZHOU Ping(周 萍), ZHOU Nai-jun(周乃君), MEI Chi(梅 炽),
CAI Qi-Feng(蔡祺风), JIANG Chang-wei(姜昌伟), WANG Zhi-qi(王志奇)
(School of Energy and Power Engineering, Central South University, Changsha 410083, China)

Abstract: The Navier-Stokes equation with the "k-ε" two-equation turbulence model was employed to describe three-dimension flow of melt in aluminum electrolysis cells. For a 160 kA cell with two current risers, the source, i.e. the electromagnetic force, in the momentum equations was solved based on the simulation results of magnetic and temperature fields. Numerical simulation on the three-dimension steady-state flow of melt was carried out. The results obtained about the velocities of molten metal on different planes, the metal/bath interface shape and the electromagnetic force distribution, were analyzed. An iron rod dissolution technique, which is based on the rate of dissolution of iron rods inserted into the melt, was used to measure the velocities of metal pad. The simulation and measurement show that there are two interaction vortexes in horizontal direction. The predictions are in well agreement with the measured results for flow pattern and velocities. It is worthwhile that in the three-dimension simulation, there is also a little change of metal velocities from level to level due to the difference of horizontal current on each level.

Key words: aluminum electrolysis cell; turbulent flow; numerical simulation; iron rod dissolution technique
CLC number: TF 821 **Document code:** A

1 INTRODUCTION

Magnetohydrodynamics (MHD) plays an important role in cell performance[1]. In recent years, not only in the new cell designing but also in increasing amperage in existing lines, more attentions have been paid on the study of MHD[2]. Two approaches have been used for determining the MHD behavior of the cells: mathematical modeling and practical measurements[3]. Many mathematical models of MHD have been proposed[4]. More rigorous models have been developed and implemented only after the computers with high speed are available. The challenges in hydrodynamics models are three-dimension flow, viscosity models and dynamic behavior, such as waves of low frequency[5]. Usual practical measurements involve magnetic field distribution, metal velocity and metal/bath interface shape using direct or indirect methods[6, 7]. A freeze profile and electric current distribution in the collector bars and anode rods are taken to determine the boundary conditions of mathematical models. The measurements are usually used to confirm the reliability and reasonableness of the mathematical models.

Calculations and measurements of metal velocities in a side-by-side cell technology, in which an 160 kA cell with two anode risers at the upstream corners is used, have been carried out. The results are reported in this paper.

2 HYDRODYNAMICS MODEL

The system consists of two liquids (electrolyte and molten aluminum), one solid (alumina) and one gas (carbon dioxide). The flow zones in the system are presented in Fig. 1.

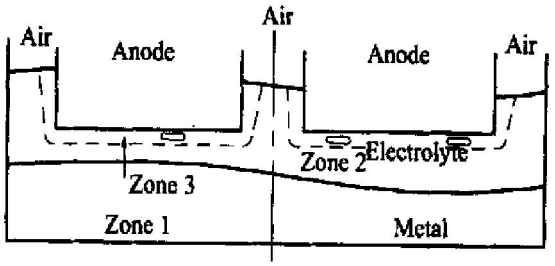

Fig. 1 Sketch of flowing space

In the electrolyte zone, there are alumina and CO_2 bubbles. At the bottom of the liquid metal, the alumina particles can be accumulated since some of them can pass through the electrolyte/metal interface to sink. Strictly speaking, therefore, the space marked by "electrolyte" is one of three-phase flow containing gas, liquid and solid. And the space marked by "metal" is one of two-phase flow involving liquid and solid. The electrolyte zone can be further divided into two zones: zone 2 and zone 3. Zone 2, which is immediately above the electrolyte/metal

① **Foundation item:** Project (G1999064900-3-2) supported by the National Key Fundamental Research and Development Program of China
Received date: 2002－01－28; **Accepted date:** 2002－05－09
Correspondence: ZHOU Ping, Zhoup@mail.csu.edu.cn

interface, is free of CO_2 bubbles. Zone 3, which is around the anode, is bubble-dominated.

Since the cell tank is made of rigid and stationary wall, internal driving forces must exist to make the fluid move. Two primary driving forces can be identified. One is the electrical and magnetic fields and the other is disturbance of bubble formed from the chemical reaction. There is the third driving force brought about by the thermal gradient. This force, however, is of less importance and can be ignored.

To simulate metal pad flow in aluminum electrolysis cells, the following assumptions were made[8].

1) The electrolyte and the metal melt are immiscible. The simulating space is confined to zone 1.

2) In the metal, any accumulation of alumina at the bottom is neglected. The two-phase flow is, therefore, reduced to a single-phase flow.

3) The metal flow is assumed to be incompressible and steady.

4) The electrolyte/metal interface is assumed to be free surface.

The fundamental physical laws applicable to describe the fluid motion in this system are the Navier-Stokes equations with the k-ε turbulent model[9].

Continuity equation:

$$\frac{\partial(\rho u_i)}{\partial x_i} = 0 \tag{1}$$

Momentum equation:

$$\frac{\partial}{\partial x_i}(\rho u_i u_j) = -\frac{\partial p}{\partial x_j} + \frac{\partial}{\partial x_i}\left[\mu_{\text{eff}}\left(\frac{\partial u_j}{\partial x_i} + \frac{\partial u_i}{\partial x_j}\right)\right] + \rho g_j + F_j \tag{2}$$

k equation:

$$\frac{\partial}{\partial x_i}(\rho k u_i) = \frac{\partial}{\partial x_i}\left[\left(\mu + \frac{\mu_T}{\sigma_k}\right)\frac{\partial k}{\partial x_i}\right] + \mu_T \frac{\partial u_j}{\partial x_i}\left(\frac{\partial u_i}{\partial x_j} + \frac{\partial u_j}{\partial x_i}\right) - \rho\varepsilon \tag{3}$$

ε equation:

$$\frac{\partial}{\partial x_i}(\rho\varepsilon u_i) = \frac{\partial}{\partial x_i}\left[\left(\mu + \frac{\mu_T}{\sigma_\varepsilon}\right)\frac{\partial \varepsilon}{\partial x_i}\right] + C_1 \frac{\varepsilon}{k}\mu_T \cdot \frac{\partial u_j}{\partial x_i}\left(\frac{\partial u_i}{\partial x_j} + \frac{\partial u_j}{\partial x_i}\right) - C_2 \rho \frac{\varepsilon^2}{k} \tag{4}$$

$$\mu_T = C_\mu \rho k^2 / \varepsilon$$

where u, x denote the velocity of liquid metal and the coordinate directions, respectively (the subscripts i, j = 1, 2, 3 refer to three coordinate directions in x, y, z), k is the turbulent kinetic energy, ε is the turbulence dissipation rate, p is pressure, ρ is metal density, g_j is the acceleration due to gravity, F_j stands for volume force (including electromagnetic force and buoyancy force), μ_{eff} is effective viscosity ($\mu_{\text{eff}} = \mu + \mu_T$, μ is the molecule viscosity and μ_T is turbulent viscosity). Furthermore, the following values were taken to be $C_\mu = 0.09$, $C_1 = 1.44$, $C_2 = 1.92$, $\sigma_k = 1.0$, $\sigma_\varepsilon = 1.3$.

The electromagnetic forces can be computed from the cross product of the electric current density, $\boldsymbol{J}$, and the magnetic induction intensity, $\boldsymbol{B}$. In terms of x, y and z components, the following expressions can be obtained:

$$F_x = J_y B_z - J_z B_y \tag{5}$$

$$F_y = J_z B_x - J_x B_z \tag{6}$$

$$F_z = J_x B_y - J_y B_x \tag{7}$$

The current density can be given with the gradients of electric potential:

$$J = -\sigma \nabla E \tag{8}$$

$$\nabla \cdot J = 0 \tag{9}$$

where E is the electric potential, σ is the electrical conductivity of melt metal. Because freezing profile influences strongly the current distribution in metal and bath, the freezing profile and magnetic field distribution are provided by simulation of temperature field and magnetic field, which, moreover, are validated by measurements.

The behavior of the interface can be derived from applying the Navier-Stokes equation to the two fluids near the interface. But in the present model the thermal and gas-driven phenomena are neglected[10]:

$$p + \rho g h = C_i \tag{10}$$

where C_i refers to a constant and h is the depth of metal.

Wall boundary conditions for the turbulence equations were treated as wall function[9]. The metal/bath interface was assumed to be a free surface and was treated approximately as a symmetry boundary[9].

3 NUMERICAL SOLUTION AND FLUID PROPERTIES

The above differential equations were discrete by applying them to each control volume in turn. The coordinate system used to represent the relevant values and coefficients is shown in Fig. 2.

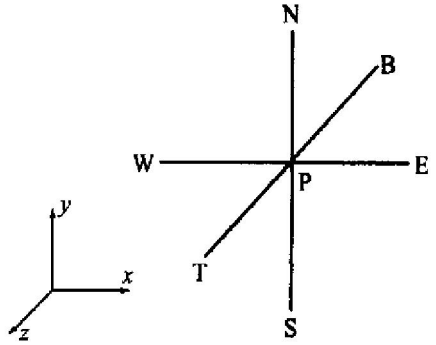

Fig. 2 Coordinate system used in numerical calculation of values and coefficients

The conservation equations in discrete form take the general form as follows:

$$\phi_p = A_N \phi_N + A_S \phi_S + A_E \phi_E + A_W \phi_W + A_T \phi_T + A_B \phi_B + B \quad (11)$$

Fig. 3(a) shows the horizontal meshes used in a 160 kA cell. The mesh consists of 71 control volumes in x direction and 21 control volumes in y direction. Fig. 3(b) gives the vertical meshes consisting of 6 domains in z direction.

The staggered grid, where the velocities are stored between the neighbor nodes and all other quantities at nodes, and the revised SIMPLE were employed[11].

The main operating parameters in a 160 kA cell and the physical properties of the molten aluminum are listed in Table 1 and 2, respectively.

Table 1 Operating parameters

Electric current/kA	Metal depth/m	Freeze profile		
		Pinch/m	Freeze height/m	Lateral toe/m
160	0.2	0.23	0.157	0.082

Table 2 Physical properties of melt metal

Density/($kg \cdot m^{-3}$)	Kinematic viscosity/($m^2 \cdot s^{-1}$)	Magnetic permeability/($H \cdot m^{-1}$)	Electric conductivity/($\Omega^{-1} \cdot m^{-1}$)
2 270	5.2×10^{-7}	$4\pi \times 10^{-7}$	3.45×10^{6}

4 RESULTS AND DISCUSSION

Fig. 4 shows a typical flow pattern in the 160 kA cell predicted by the model. It can be seen from this figure that there are two interconnected flow loops. The loops locate at the left and right sides of the longitudinal centerline of the cell. One near the tap end is slightly greater than the other near the duct end. The maximum velocity is 0.182 8 m/s and the average velocity is 0.095 4 m/s. Also, according to the distribution tendency of metal velocity demonstrated in Fig. 4, the average velocity at the downstream side is higher than that at the upstream side, and the velocity at the tap end is higher than that at the duct end. There is a zone with small velocities in the vicinity of the upstream and downstream sides between anode 6 and anode 7(The number of anodes are referred to Fig. 5). The main zones with higher velocities are near the downstream side, duct end and tap end.

The measurements of metal velocity at 18 points were carried out using an iron rod dissolution method. The locations measured are shown in Fig. 5. The velocities of liquid metal are measured three times at the same cell, and each time spends 8 min. Therefore, three groups of data can be gotten and shown in Fig. 5 with different linetype array. The direction of array denotes flow direction of metal, and the length of array denotes the magnitude of velocity, which is the average value of three measurements. The maximum velocity obtained is 0.179 m/s and the average value is 0.143 1 m/s. Two vortexes are also revealed according to the direction of arrays of measured results(as shown in Fig. 5).

It can be seen from Figs. 4 and 5 that the calculated results about the flow patterns and the values of velocity are essentially in agreement with those measured.

It is found in the three-dimension simulations that there are also some discrepancies of velocities in the ver-

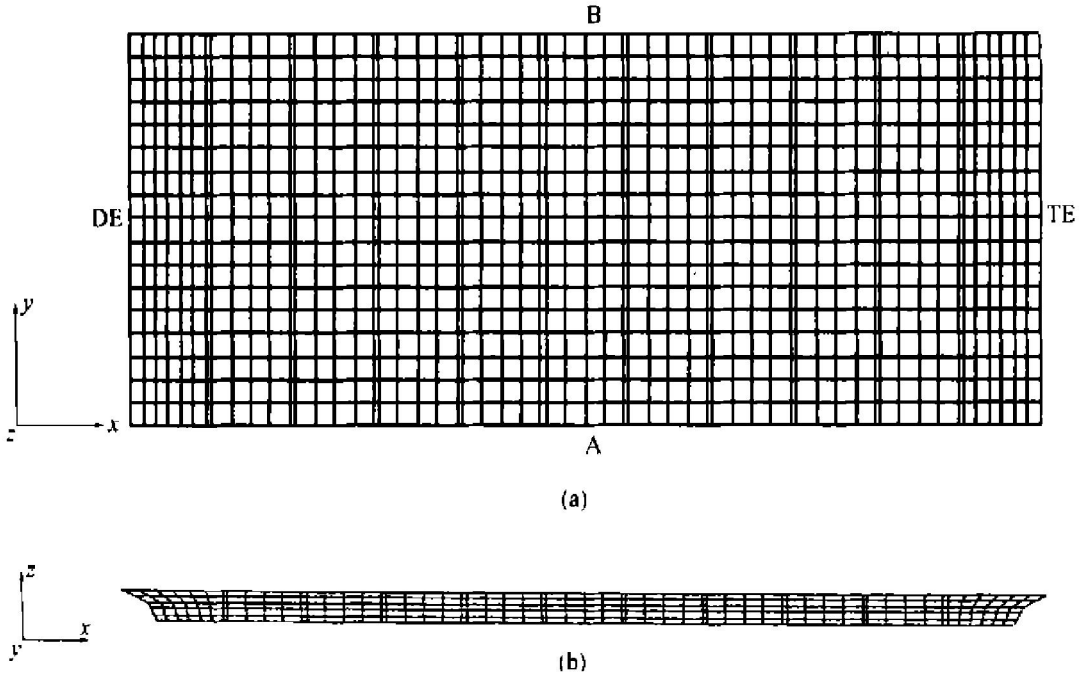

Fig. 3 Mesh distribution for a 160 kA cell
(a) —Horizontal meshes; (b) —Vertical meshes in longitudinal direction

tical section(as shown in Fig. 6), but the changes from level to level are very consistent and reasonable, which are influenced by different friction forces and current distribution. This is just the difference between three-dimension and quasi three-dimension simulation. It is worthwhile to point out that the length of array in Fig. 6 doesn't represent the real value of velocity, because this is only the project of velocity vector on the vertical plane.

Fig. 7 shows the electromagnetic force distribution in the horizontal direction. It can clearly be seen that the distribution is asymmetrical. The force at the upstream side is greater than that at the downstream side. The electromagnetic force drives the liquid metal to move towards the center of the cell at the upstream side, and then diverge from the center at the downstream side, thus, forming two vortexes. The maximum intensity of the force is 67 N/m^3.

Fig. 8 presents the metal/bath interface shape. The maximum height of the interface is 0. 21 m, and the minimum is 0. 175 m. It is obvious that the interface is in a form of wave.

5 CONCLUSION

The two methods of simulation and measurement for the velocity of liquid metal in the electrolysis cells presented here are valuable for evaluating of the cell. The validity of the three-dimension mathematical model and the simulation technique has been confirmed in the present work, which can be used for optimizing the design and operation of cells.

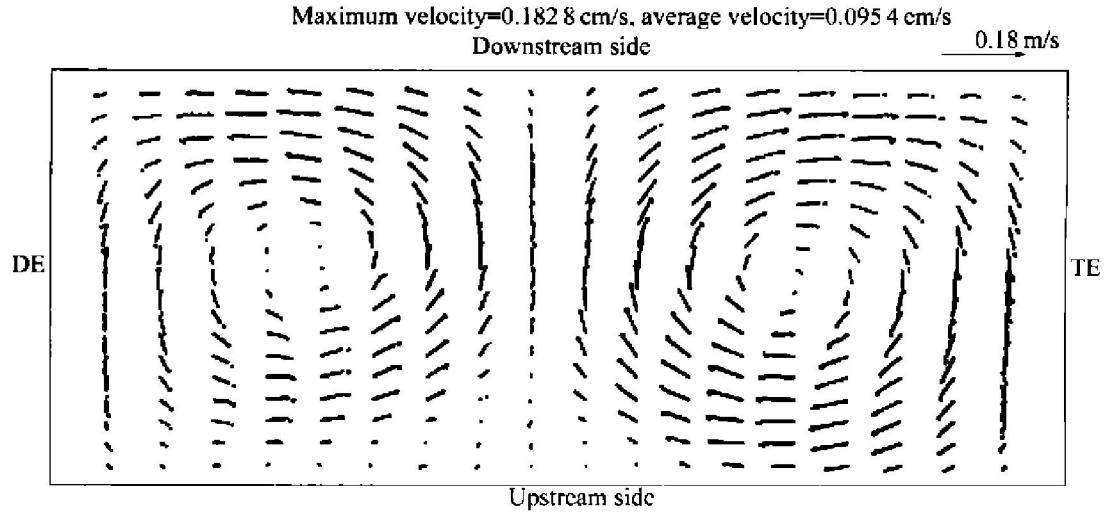

Fig. 4 Predicted metal flow pattern on horizontal plane

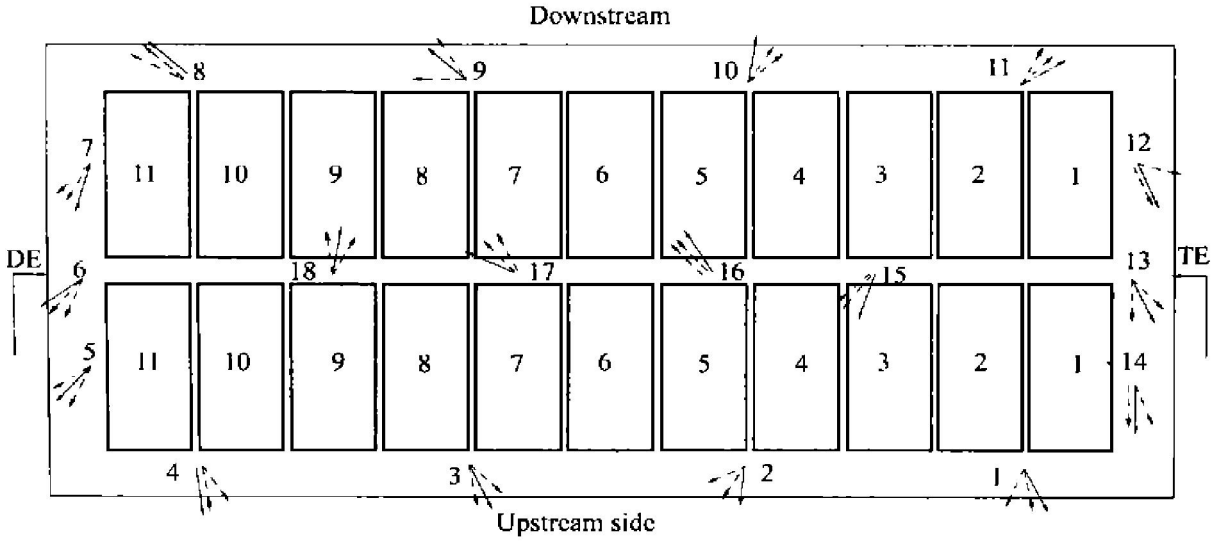

Fig. 5 Measured metal velocity on horizontal plane

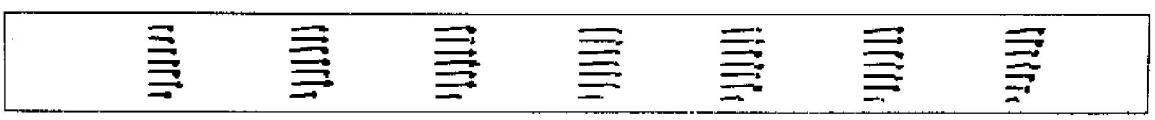

Fig. 6 Predicted metal flow pattern on vertical plane in transverse direction

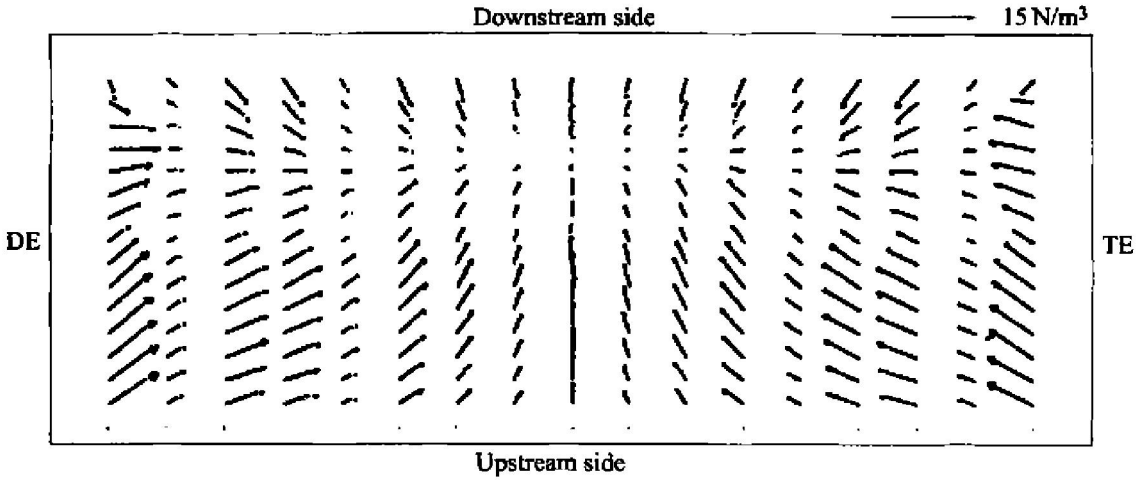

Fig. 7 Predicted horizontal electromagnetic force distribution

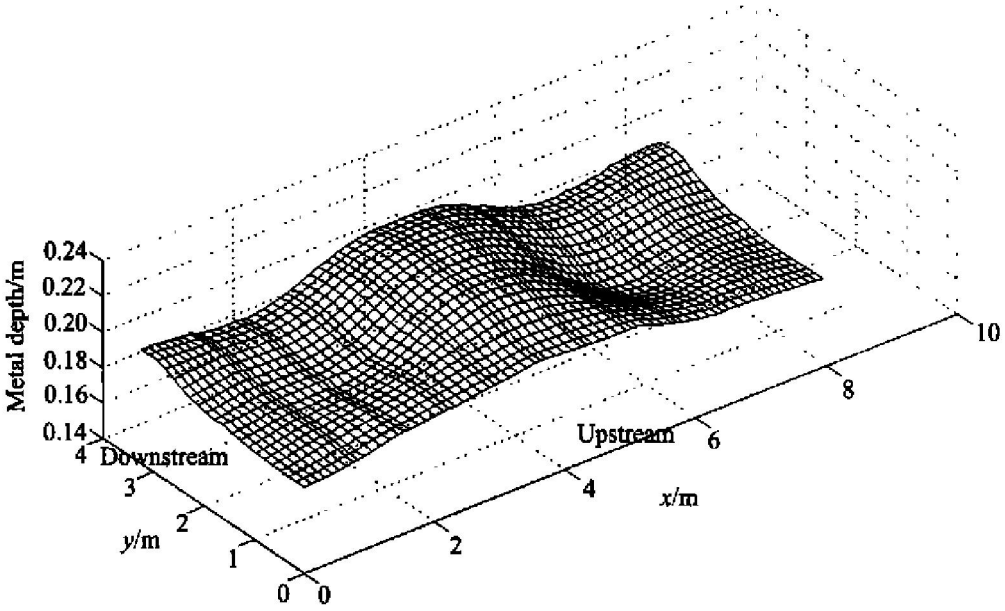

Fig. 8 Predicted metal/bath interface shape

REFERENCES

[1] Potocnik V. Principles of MHD design of aluminum electrolysis cells[A]. Cutdshall E R. 121th TMS Annual Meeting, Light Metals[C]. San Diego, California, 1992. 1187-1193.

[2] Antille J, Von Kaenel R. Busbar optimization using cell stability criteria and its impact on cell performance[A]. Edward E C. 128th TMS Annual Meeting, Light Metals[C]. San Diego, California, 1999, 165-170.

[3] Potocnik V, Laroche F. Comparison of measured and calculated metal pad velocities for different prebake cell designs[A]. Anjier J L. 130th TMS Annual Meeting, Light Metals[C]. New Orleans, Louisiana, 2001. 419-425.

[4] HUANG Zhao-lin, YANG Zhi-feng, WU Jiang-hang. Numerical simulation of turbulent flow and interface wave in aluminum reduction cell[J]. Chinese Journal of Computational Physics, 1994, 11(2): 179-183. (in Chinese)

[5] MEI Chi. Simulation and Optimization of Non-Ferrous Metallurgical Furnaces[M]. Beijing: Metallurgy Industry Press, 2001. 72. (in Chinese)

[6] Ziegler D P, Kozarek R L. Hall-Heroult cell magnetic measurements and comparisons with calculations[A]. Rooy E L. 120th TMS Annual Meeting, Light Metals[C]. New Orleans, Louisiana, 1991, 381-391.

[7] Pant A, Langille A, Roy R. Measurement of liquid metal flow velocities in electrolytic cells: test of the iron rod method [A]. Miller R E. 115th TMS Annual Meeting, Light Metals [C]. New Orleans, Louisiana, 1986. 541-550.

[8] Ai D K. The hydrodynamics of the Hall-Heroult cell: an overview[A]. Bohner H O. 114th TMS Annual Meeting, Light Metals[C]. New York, 1985. 593-607.

[9] QIN Ke-fa, FAN Jian-ren. Theory and Calculation of Gas-Solid Multi-phase Flow in Engineering[M]. Hangzhou: Zhejiang University Press, 1990. 60. (in Chinese)

[10] Wahnsiedler W E. Hydrodynamic modeling of commercial Hall-Heroult cells[J]. Zabreznik R D. 116th TMS Annual Meeting, Light Metals[C]. Colorado, 1987. 269-287.

[11] Patankar S V. Numerical Heat Transfer and Fluid Flow [M]. US: Hemisphere Publishing Corporation, 1980. 146. (in Chinese)

(Edited by YANG Bing)